

Supplementary Information for

The energy gap law for NIR-phosphorescent Cr(III) complexes

Yang Cheng,^a Qingqing Yang,^a Jiang He,^a Wenjie Zou,^a Keyu Liao,^a Xiaoyong Chang,^a Chao Zou,^{*ab} and Wei Lu^{*a}

Department of Chemistry, Southern University of Science and Technology, Shenzhen, Guangdong 518055, P. R. China. E-mail: luw@sustech.edu.cn.

Functional Coordination Material Group-Frontier Research Center, Songshan Lake Materials Laboratory, Dongguan, Guangdong 523808, P. R. China. Email: zouchao@sslab.org.cn.

Table of Contents

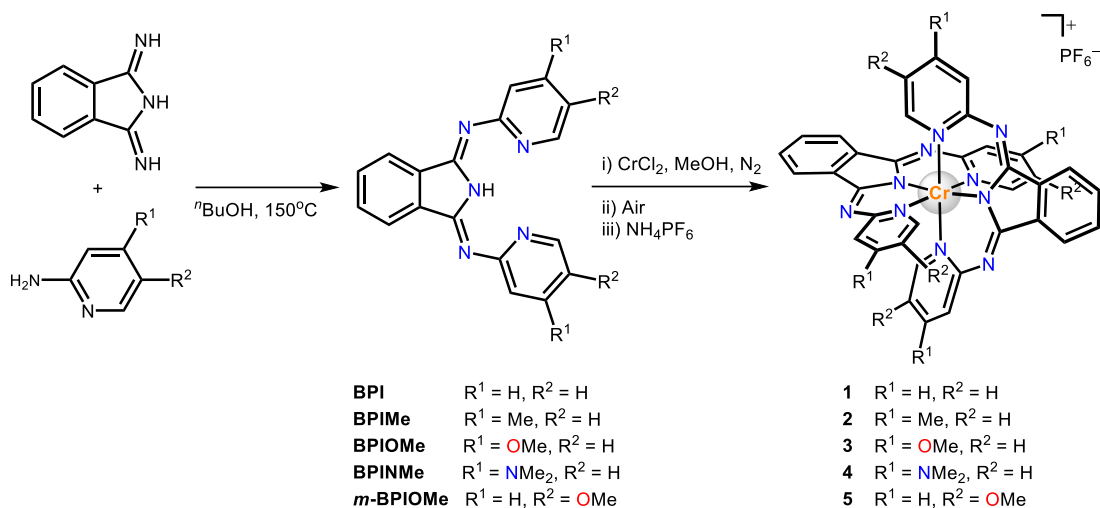
1. General procedures
2. Synthesis and characterization of the ligands and Cr(III) complexes
3. NMR spectra
4. Mass spectra
5. X-ray crystallography
6. EPR spectra for the Cr(III) complexes
7. Photophysical properties
8. References

General Procedures. All starting materials were purchased from commercial sources and used without further purification. Solvents were of analytical grade unless stated otherwise. Manipulations and synthesis of all metal complexes were performed inside a dinitrogen-filled glovebox (MBRAUN Labmaster 130). ^1H and ^{13}C NMR spectra were recorded on Bruker Avance III 400M or 500 M spectrometers. HR-MS (high resolution mass) spectra were obtained on a Thermo Scientific Q Exactive mass spectrometer. Low resolution mass spectra were obtained on a Thermo Scientific LCQ Fleet. Elemental analyses were performed on the Elementar vario EL cube. X-ray photoelectron spectroscopy (XPS) spectra were recorded using a ULVAC PHI 5000 VersaProbe III system equipped with an Al K α X-ray source. Electron paramagnetic resonance (EPR) were performed with Bruker EMXplus-10/12 spectrometer on a frozen CH₃CN solution at 100 K. Infrared (IR) spectra were obtained by Bruker Vertex 70v. UV-Vis absorption spectra were recorded on a Thermo Scientific Evolution 201 UV-Visible Spectrophotometer. Emission spectra and lifetime measurements were performed via Edinburg spectrometer FLS-980 equipped with MCP-PMT and NIR-PMT detectors. Absolute luminescent quantum yields were recorded with Hamamatsu absolute PL quantum yield spectrometer C11347. Relative luminescent quantum yields were calculated according to Equation (1),

$$\Phi_S = \Phi_R \times \frac{I_S}{I_R} \times \frac{A_R}{A_S} \times \left(\frac{n_S}{n_R} \right)^2 \quad (1)$$

The subscripts S and R denote the sample and reference respectively. Φ_R is the known quantum yield of the reference standard, I is the integrated photoluminescence intensity in the emission spectrum (measured with acetonitrile solutions under the identical instrumental set-ups), A is the absorbance of the solution at the excitation wavelength (λ_{ex}), and n is the refractive index of the solvent. Given that the same solvent (acetonitrile) was used for both the reference and the samples, the refractive index term can be eliminated. Absolute emission quantum yield of complex **4** in degassed acetonitrile was recorded with an integrating sphere and those of **1–3** and **5** were obtained with a relative method using **4** as the reference. Time-resolved transient absorption spectra were recorded with Edinburgh

LP-920 Laser Flash Photolysis Spectrometer equipped with an ICCD detector. Electrochemical studies were carried out using CHI-620E electrochemical workstation. A three-electrode system was used which consisted of a glassy carbon disk working electrode, Ag/AgCl reference and a Pt-wire counter electrode. Cyclic voltammetry (CV) and differential pulse voltammetry (DPV) were performed in CH₃CN with 0.1 M ⁿBu₄NPF₆ (recrystallized from ethanol and dried in vacuum at 80 °C) as supporting electrolyte at 298 K (scan rates: 50 mV/s). Ferrocene (Fc) was used as the internal reference. UV-vis-NIR spectro-electrochemical measurement of complexes **1–5** (1×10⁻⁴ M in CH₃CN) recorded at 298 K, indium tin oxide (ITO) glass substrates as working electrode.



Scheme S1. Synthesis of the ligands and Cr(III) complexes.

Ligands were prepared according to the published method with minor modifications.¹⁻⁴

Synthesis of ligand BPI

A mixture of 1,3-diiminoisoindoline (1.45 g, 10 mmol) and excess 2-aminopyridine (2.07 g, 22 mmol) in *n*-butanol (30 mL) was stirred under reflux for 18 h under N₂ atmosphere. After cooling to room temperature, the resulting solution was evaporated to dryness. Then the residue was redissolved in dichloromethane and

purified by column chromatography (ethyl acetate:dichloromethane, 1:4 as eluent) to give green fibrous solid (1.39 g, 47%). MS: *m/z* 300.23 (calculated for [M + H]⁺ 300.12). ¹H NMR (400 MHz, CDCl₃): δ 14.16 (s, 1H), 8.68–8.58 (m, 2H), 8.19 (s, 2H), 7.80 (td, *J* = 7.9, 1.7 Hz, 2H), 7.68 (dd, *J* = 5.4, 3.0 Hz, 2H), 7.57 (s, 2H), 7.22–7.10 (m, 2H) ppm.

Synthesis of ligand BPIMe

A mixture of 1,3-diiminoisoindoline (1.45 g, 10 mmol) and excess 2-amino-4-methylpyridine (2.38 g, 22 mmol) in *n*-butanol (30 mL) was stirred under reflux for 18 h under N₂ atmosphere. After cooling to room temperature, the resulting solution was evaporated to dryness. Then the residue redissolved in dichloromethane and purified by column chromatography (petroleum ether:dichloromethane, 1:5 as eluent) to give yellow green fibrous solid (1.67 g, 51%). MS: *m/z* 328.31 (calculated for [M + H]⁺ 328.16). ¹H NMR (400 MHz, DMSO-*d*₆): δ 13.98 (s, 1H), 8.55 (d, *J* = 5.0 Hz, 2H), 8.01 (dt, *J* = 6.7, 3.4 Hz, 2H), 7.79–7.72 (m, 2H), 7.30 (s, 2H), 7.14–7.08 (m, 2H), 2.38 (s, 6H) ppm.

Synthesis of ligand precursor BPIOMe

A mixture of 1,3-diiminoisoindoline (1.45 g, 10 mmol) and excess 2-amino-4-methoxypyridine (2.73 g, 22 mmol) in *n*-butanol (30 mL) was stirred under reflux for 12 h under N₂ atmosphere. After cooling to room temperature, the resulting solution was evaporated to dryness. Then the residue redissolved in dichloromethane and purified by column chromatography (ethyl acetate:dichloromethane, 1:2 as eluent) to give yellow fibrous solid (2.43 g, 68%). MS: *m/z* 360.22 (calculated for [M + H]⁺ 360.15). ¹H NMR (400 MHz, CDCl₃): δ 8.40 (d, *J* = 5.8 Hz, 2H), 8.15 (s, 2H), 7.67 (dd, *J* = 5.5, 3.0 Hz, 2H), 7.07 (s, 2H), 6.71 (dd, *J* = 5.8, 2.4 Hz, 2H), 3.92 (s, 6H) ppm.

Synthesis of ligand precursor BPINMe₂

A mixture of 1,3-diiminoisoindoline (1.45 g, 10 mmol) and excess 2-amino-4-(dimethylamino)pyridine (3.02 g, 22 mmol) in *n*-butanol (30 mL) was stirred under

reflux for 36 h under N₂ atmosphere. After cooling to room temperature, the resulting solution was evaporated to dryness. Then the residue redissolved in dichloromethane and purified by column chromatography (methanol:dichloromethane, 1:30 as eluent) to give yellow fibrous solid (417 mg, 11%). MS: *m/z* 386.33 (calculated for [M + H]⁺ 386.21). ¹H NMR (400 MHz, CDCl₃): δ 8.24 (d, *J* = 6.0 Hz, 2H), 8.08 (s, 2H), 7.62 (dq, *J* = 7.0, 4.0 Hz, 2H), 6.71 (s, 2H), 6.38 (dd, *J* = 6.0, 2.5 Hz, 2H), 3.06 (s, 12H) ppm.

Synthesis of ligand precursor *m*-BPIOMe

A mixture of 1,3-diiminoisoindoline (1.45 g, 10 mmol) and excess 2-amino-5-methoxypyridine (2.73 g, 22 mmol) in *n*-butanol (30 mL) was stirred under reflux for 12 h under N₂ atmosphere. After cooling to room temperature, the resulting solution was evaporated to dryness. Then the residue redissolved in dichloromethane and purified by column chromatography (methanol:dichloromethane, 1:100 as eluent) to give yellow solid (2.64 g, 73%). MS: *m/z* 360.31 (calculated for [M + H]⁺ 360.15). ¹H NMR (500 MHz, CDCl₃): δ 13.89 (s, 1H), 8.29 (d, *J* = 3.1 Hz, 2H), 8.14–8.01 (m, 2H), 7.62 (dd, *J* = 5.5, 3.0 Hz, 2H), 7.45 (d, *J* = 8.7 Hz, 2H), 7.31 (dd, *J* = 8.7, 3.1 Hz, 2H), 3.92 (s, 6H) ppm. ¹³C{¹H} NMR (126 MHz, CDCl₃) δ 153.88, 153.34, 152.31, 135.55, 134.87, 131.57, 123.75, 122.95, 122.63, 56.08 (OMe) ppm.

Synthesis of [Cr(BPI)₂]PF₆ (1)

To a solution of BPI (365 mg, 1.219 mmol) in deaerated methanol (30 mL) was added anhydrous chromium(II) chloride (100 mg, 0.814 mmol in deaerated methanol (10 mL)) and kept stirring for 72 h under N₂ atmosphere at room temperature. After that, the mixture was left under air for stirring another 2 h. The resulting mixture was then filtered, and the collected organic layer was added to a solution of NH₄PF₆ (663 mg, 4.064 mmol) in deionized water. An orange solid precipitated out from the solution and the solid was collected by filtration. The solid was then washed with water (3×15 mL) and further purified by recrystallization from acetonitrile (dark red crystals, 83 mg, 17%). Anal. Calcd for C₃₆H₂₄N₁₀CrPF₆: C, 54.48; H, 3.05; N, 17.65; Found: C, 54.29;

H, 2.924; N, 17.44. HR-MS: m/z 648.1567 (calculated for $[\text{Cr}(\text{BPI})_2]^+$ 648.1591).

Synthesis of $[\text{Cr}(\text{BPIMe})_2]\text{PF}_6$ (2)

To a solution of BPIMe (400 mg, 1.222 mmol) in deaerated methanol (30 mL) was added anhydrous chromium(II) chloride (100 mg, 0.814 mmol in deaerated methanol (10 mL)) and kept stirring for 72 h under N_2 atmosphere at room temperature. After that, the mixture was left under air for stirring another 2 h. The resulting mixture was then filtered, and the collected organic layer was added to a solution of NH_4PF_6 (663 mg, 4.064 mmol) in deionized water. An orange solid precipitated out from the solution and the solid was collected by filtration. The solid was then washed with water (3×15 mL) and further purified by column chromatography (methanol:dichloromethane, 1:50 as eluent) and recrystallized from petroleum ether/dichloromethane (red crystals, 107 mg, 21%). Anal. Calcd for $\text{C}_{40}\text{H}_{32}\text{N}_{10}\text{CrPF}_6$: C, 56.54; H, 3.80; N, 16.48; Found: C, 56.61; H, 3.442; N, 16.61. HR-MS: m/z 704.2201 (calculated for $[\text{Cr}(\text{BPIMe})_2]^+$ 704.2217).

Synthesis of $[\text{Cr}(\text{BPIOMe})_2]\text{PF}_6$ (3)

To a solution of BPIOMe (439 mg, 1.222 mmol) in deaerated methanol (30 mL) was added anhydrous chromium(II) chloride (100 mg, 0.814 mmol in deaerated methanol (10 mL)) and kept stirring for 72 h under N_2 atmosphere at room temperature. After that, the mixture was left under air for stirring another 2 h. The resulting mixture was then filtered, and the collected organic layer was added to a solution of NH_4PF_6 (663 mg, 4.064 mmol) in deionized water. An orange solid precipitated out from the solution and the solid was collected by filtration. The solid was then washed with water (3×15 mL) and further purified by recrystallization from acetonitrile (red crystals, 129 mg, 23%). Anal. Calcd for $\text{C}_{40}\text{H}_{32}\text{N}_{10}\text{O}_4\text{CrPF}_6$: C, 52.58; H, 3.53; N, 15.33; Found: C, 52.93; H, 3.323; N, 15.59. HRMS: m/z 768.1992 (calculated for $[\text{Cr}(\text{BPIOMe})_2]^+$ 768.2013).

Synthesis of $[\text{Cr}(\text{BPINMe}_2)_2]\text{PF}_6$ (4)

To a solution of BPINMe₂ (235 mg, 0.610 mmol) in deaerated methanol (20 mL) was added anhydrous chromium(II) chloride (50 mg, 0.407 mmol in deaerated methanol (10 mL)) and kept stirring for 72 h under N₂ atmosphere at room temperature. After that, the mixture was left under air for stirring another 2 h. The resulting mixture was then filtered, and the collected organic layer was added to a solution of NH₄PF₆ (332 mg, 2.037 mmol) in deionized water. An orange solid precipitated out from the solution and the solid was collected by filtration. The solid was then washed with water (3×15 mL) and further purified by column chromatography (methanol:dichloromethane, 1:25 as eluent) and recrystallized from petroleum ether/dichloromethane (orange crystals, 56 mg, 19%). Anal. Calcd for C₄₄H₄₄N₁₄CrPF₆: C, 54.71; H, 4.59; N, 20.30; Found: C, 53.78; H, 4.419; N, 19.97. HRMS: *m/z* 820.3264 (calculated for [Cr(BPINMe₂)₂]⁺ 820.3278).

Synthesis of [Cr(*m*-BPIOMe)₂]PF₆ (5)

To a solution of *m*-BPIOMe (439 mg, 1.222 mmol) in deaerated methanol (30 mL) was added anhydrous chromium(II) chloride (100 mg, 0.814 mmol in deaerated methanol (10 mL)) and kept stirring for 72 h under N₂ atmosphere at room temperature. After that, the mixture was left under air for stirring another 2 h. The resulting mixture was then filtered, and the collected organic layer was added to a solution of NH₄PF₆ (663 mg, 4.064 mmol) in deionized water. An orange solid precipitated out from the solution and the solid was collected by filtration. The solid was then washed with water (3×15 mL) and further purified by column chromatography (methanol:dichloromethane, 1:30 as eluent) and recrystallized from petroleum ether/dichloromethane (dark red crystals, 151 mg, 27%). Anal. Calcd for C₄₀H₃₂N₁₀O₄CrPF₆: C, 52.58; H, 3.53; N, 15.33; Found: C, 52.54; H, 3.345; N, 15.34. HRMS: *m/z* 768.1994 (calculated for [Cr(*m*-BPIOMe)₂]⁺ 768.2013).

NMR Spectra

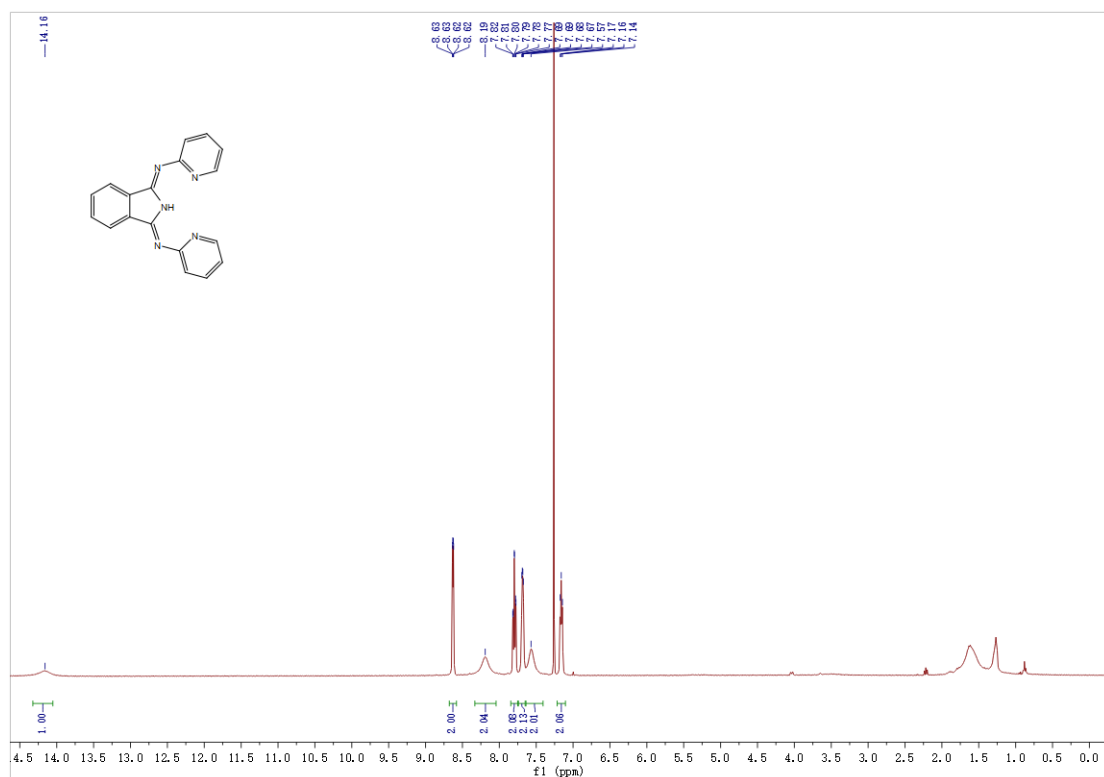


Figure S1. ¹H NMR spectrum of BPI (400 MHz, CDCl₃).

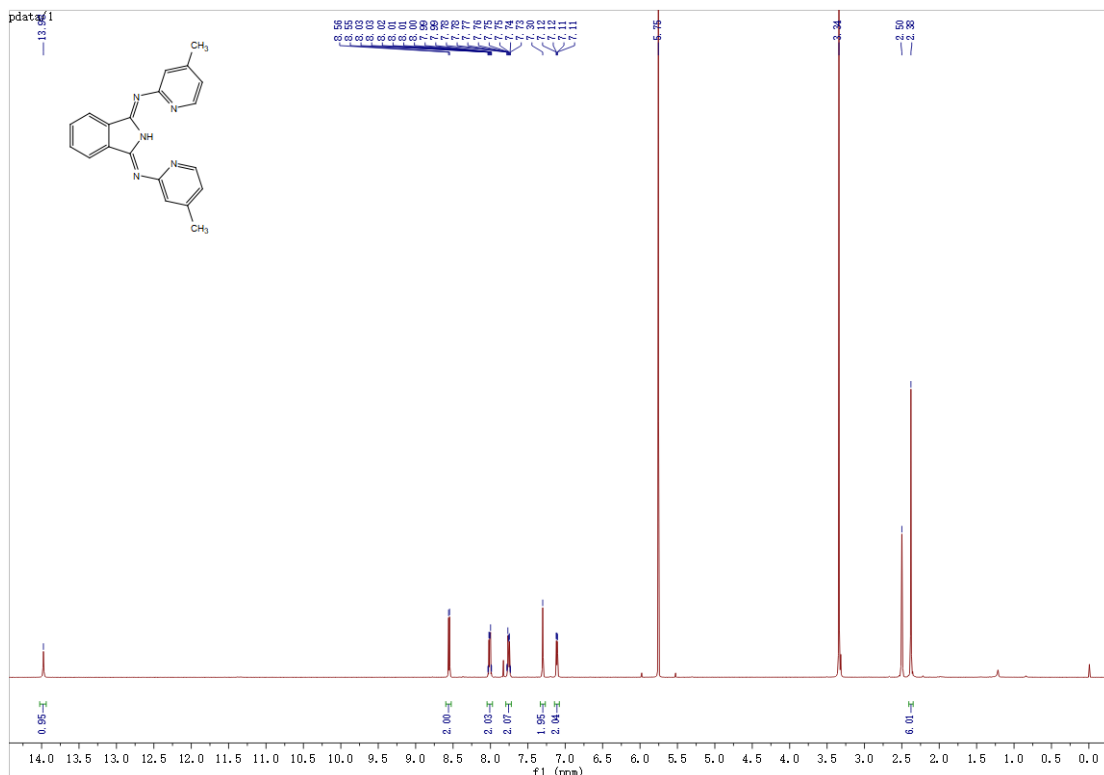


Figure S2. ¹H NMR spectrum of BPIMe (400 MHz, DMSO-d₆).

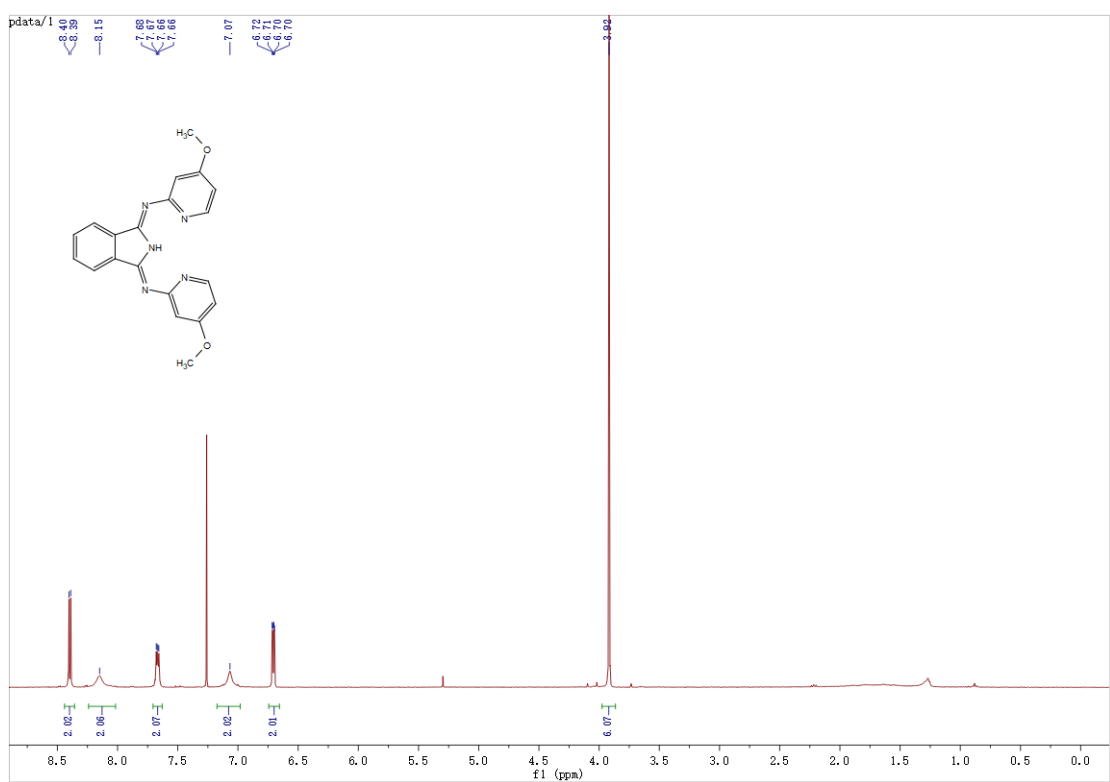


Figure S3. ¹H NMR spectrum of BPIOMe (400 MHz, CDCl₃).

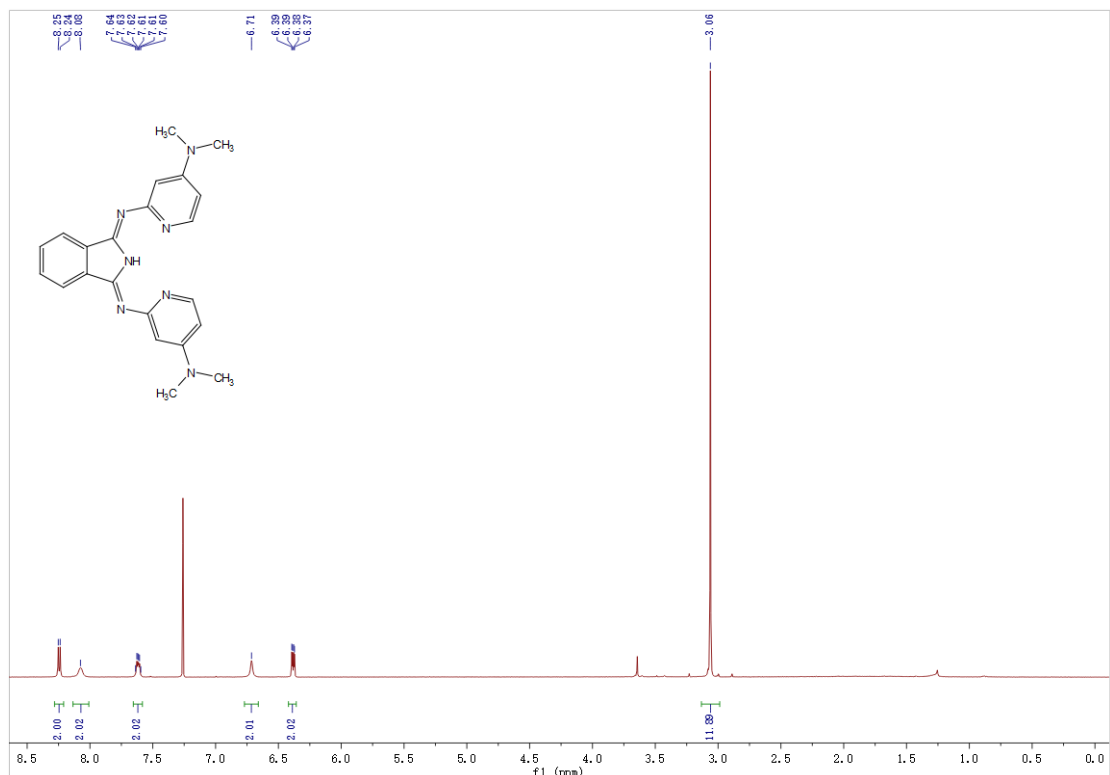


Figure S4. ¹H NMR spectrum of BPINMe₂ (400 MHz, CDCl₃).

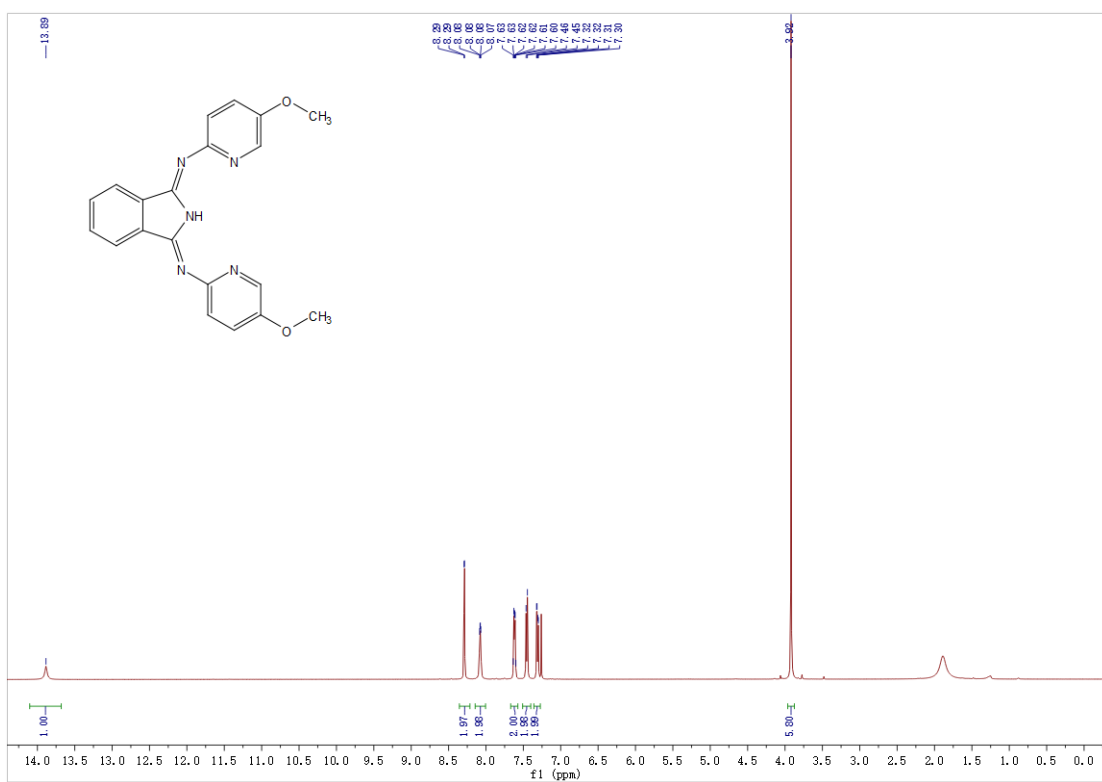


Figure S5. ^1H NMR spectrum of *m*-BPIOMe (500 MHz, CDCl_3).

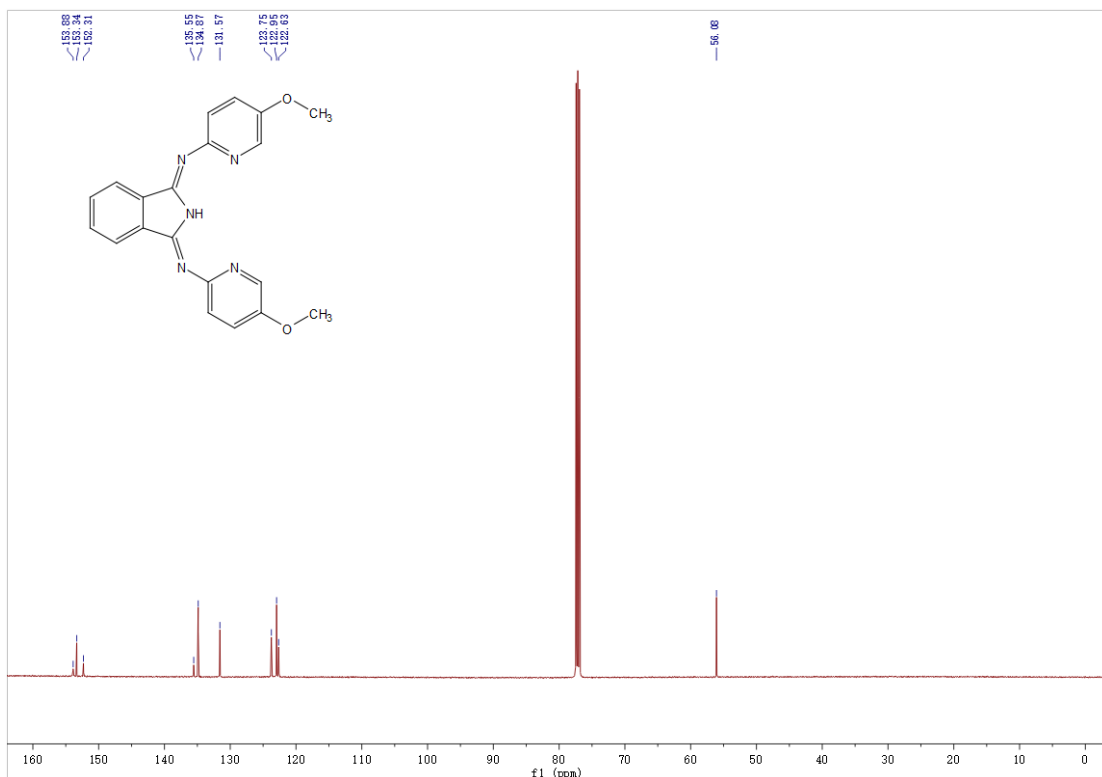


Figure S6. $^{13}\text{C}\{^1\text{H}\}$ NMR spectrum of *m*-BPIOMe (126 MHz, CDCl_3).

Mass spectra

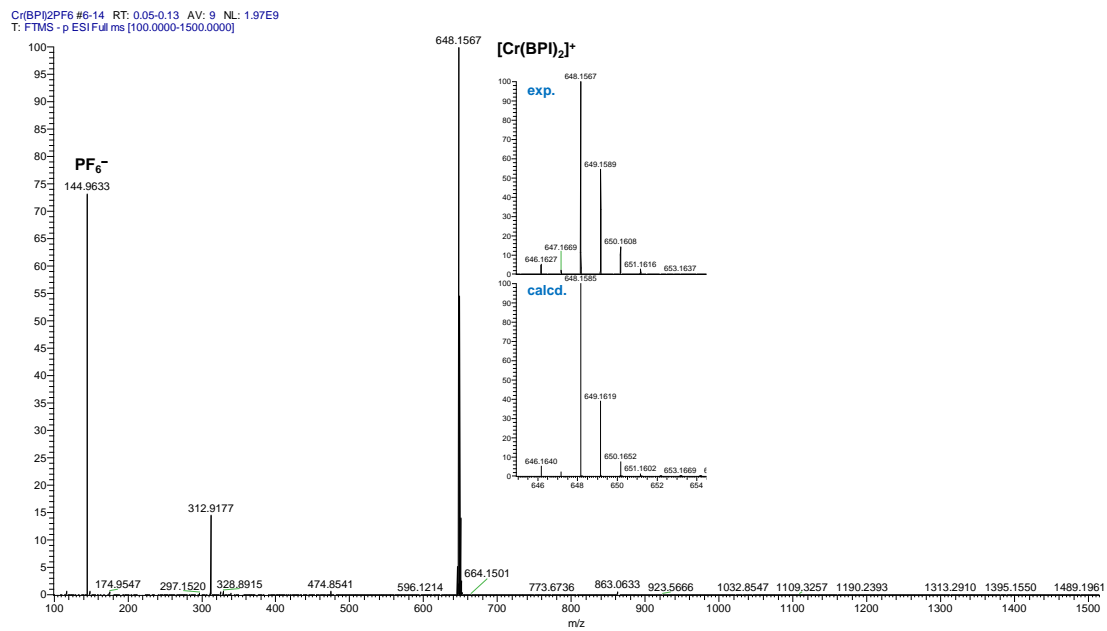


Figure S7. HR-MS (ESI) mass spectrum of [Cr(BP)₂]PF₆ (**1**). The insets depict the experimental (top) and calculated (bottom) isotopic pattern of the peak.

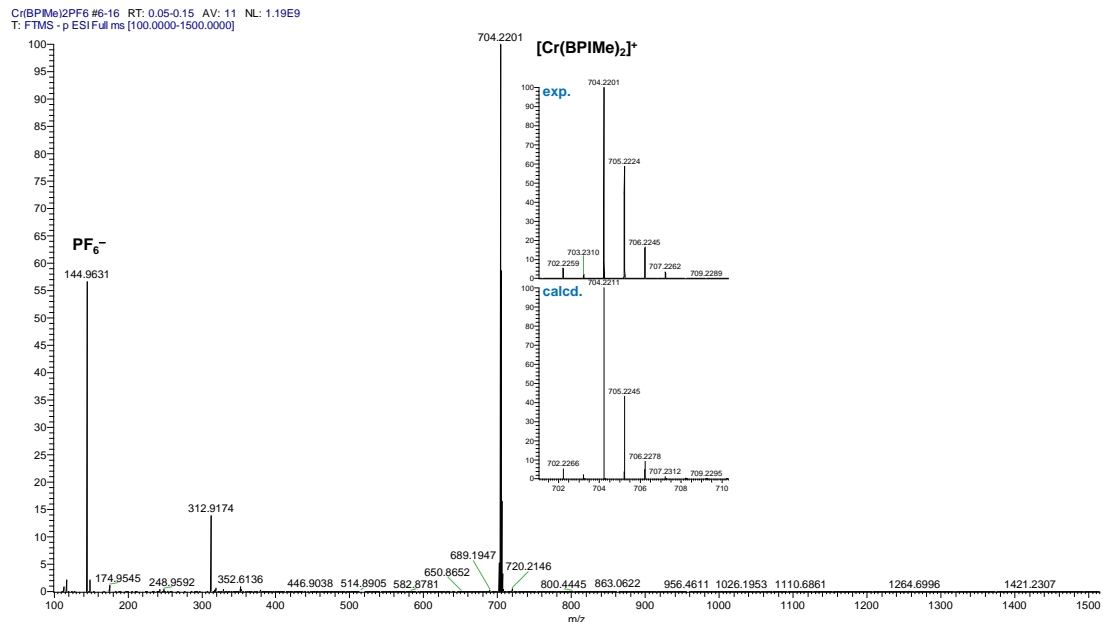


Figure S8. HR-MS (ESI) mass spectrum of [Cr(BPIMe)₂]PF₆ (**2**). The insets depict the experimental (top) and calculated (bottom) isotopic pattern of the peak.

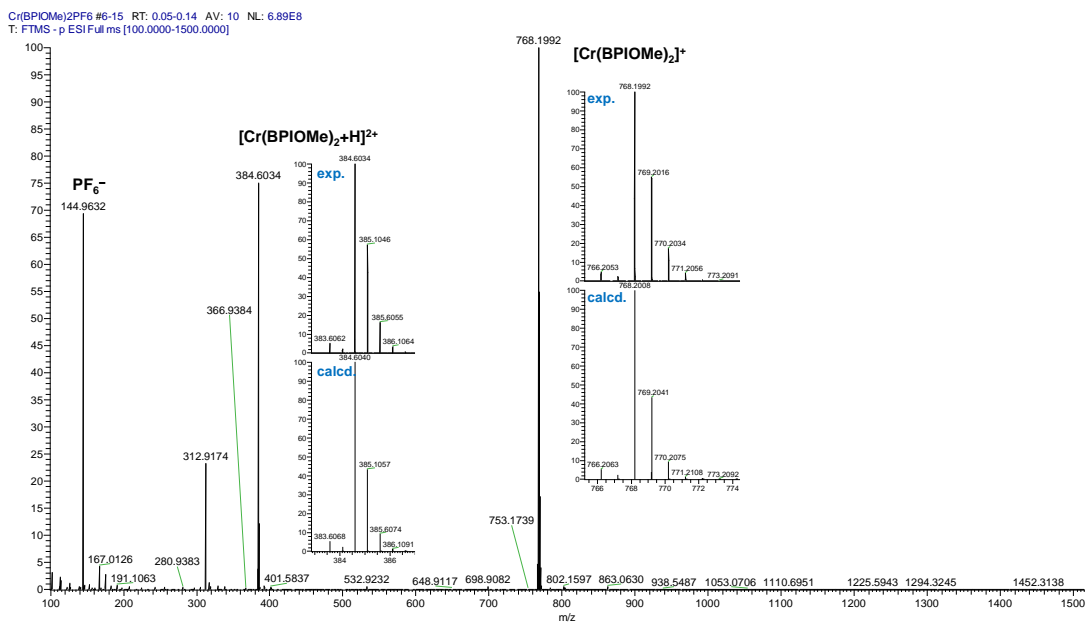


Figure S9. HR-MS (ESI) mass spectrum of $[\text{Cr}(\text{BPIMe})_2]\text{PF}_6$ (**3**). The insets depict the experimental (top) and calculated (bottom) isotopic pattern of the peak.

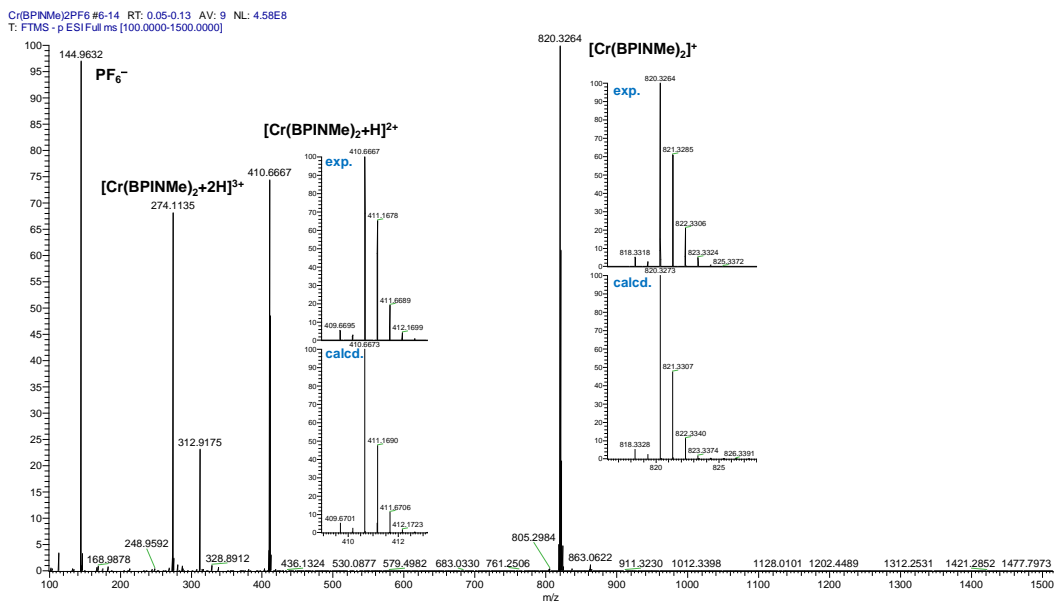


Figure S10. HR-MS (ESI) mass spectrum of $[\text{Cr}(\text{BPINMe})_2]\text{PF}_6$ (**4**). The insets depict the experimental (top) and calculated (bottom) isotopic pattern of the peak.

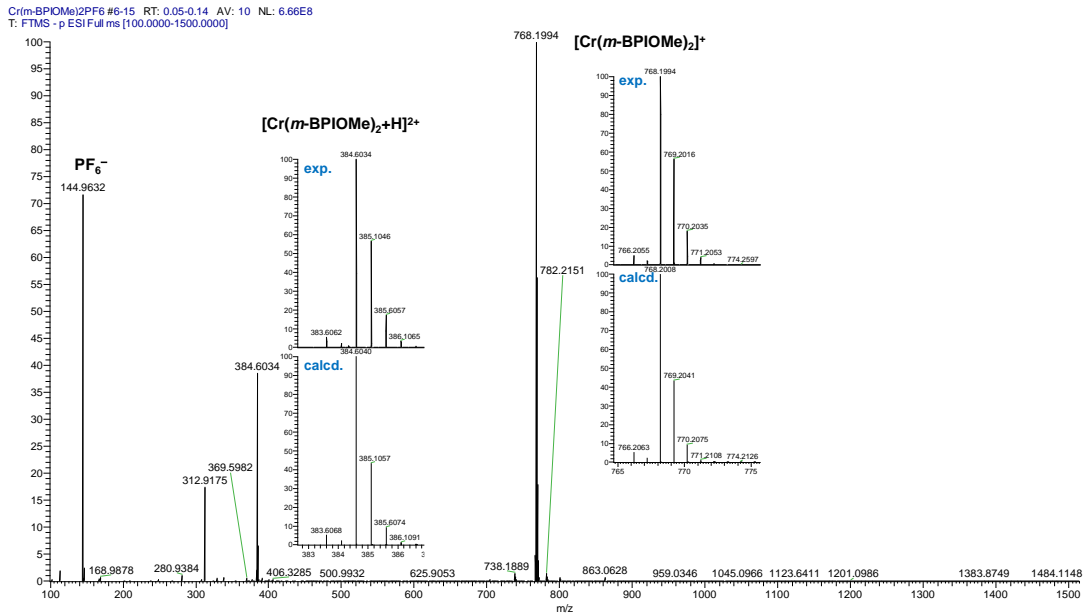


Figure S11. HR-MS (ESI) mass spectrum of $[\text{Cr}(m\text{-BPIOMe})_2]\text{PF}_6$ (**5**). The insets depict the experimental (top) and calculated (bottom) isotopic pattern of the peak.

X-ray crystallography. Single crystals of complexes **2**, **4** and **5** which suitable for X-ray diffraction studies were obtained by slow diffusion of n-hexane into a saturated CH_2Cl_2 solution of corresponding Cr complexes. Singles crystal of complexes **1** and **3** were obtained by slow evaporation of a saturated CH_3CN solution of corresponding Cr complexes. Suitable crystals were selected and detected on a Bruker D8 VENTURE diffractometer. The crystals were kept at 100 K during data collection. Using Olex²⁵, the structure was solved with the SHELXT⁶ structure solution program using Intrinsic Phasing and refined with the SHELXL⁷ refinement package using Least Squares minimisation.

Table S1. Crystallographic parameters for the structure of [Cr(BPI)₂]PF₆ (**1**).

Empirical formula	C ₃₆ H ₂₄ CrF ₆ N ₁₀ P
Formula weight	793.62
Temperature/K	100
Crystal system	orthorhombic
Space group	Pbcn
a/Å	12.2442(12)
b/Å	32.934(3)
c/Å	8.7564(7)
α/°	90
β/°	90
γ/°	90
Volume/Å ³	3531.0(6)
Z	4
ρ _{calc} g/cm ³	1.493
μ/mm ⁻¹	3.755
F(000)	1612
Crystal size/mm ³	0.35 × 0.32 × 0.002
Radiation	CuKα (λ = 1.54178)
2θ range for data collection/°	5.366 to 118.956
Index ranges	-13 ≤ h ≤ 13, -25 ≤ k ≤ 36, -9 ≤ l ≤ 9
Reflections collected	14739
Independent reflections	2547 [R _{int} = 0.0973, R _{sigma} = 0.0651]
Data/restraints/parameters	2547/12/245
Goodness-of-fit on F ²	1.179
Final R indexes [>=2σ (I)]	R ₁ = 0.1936, wR ₂ = 0.4354
Final R indexes [all data]	R ₁ = 0.2018, wR ₂ = 0.4383
Largest diff. peak/hole / e Å ⁻³	0.86/-1.02

Table S2. Crystallographic parameters for the structure of [Cr(BPIMe)₂]PF₆ (**2**).

Empirical formula	C _{41.13} CrF ₆ H _{37.51} N ₁₀ O _{1.63} P
Formula weight	894.93
Temperature/K	100
Crystal system	monoclinic
Space group	P2 ₁ /c
a/Å	19.9874(13)
b/Å	18.8599(12)
c/Å	21.5414(14)
α/°	90
β/°	102.640(2)
γ/°	90
Volume/Å ³	7923.5(9)
Z	8
ρ _{calc} g/cm ³	1.5
μ/mm ⁻¹	0.408
F(000)	3683
Crystal size/mm ³	0.33 × 0.32 × 0.28
Radiation	MoKα (λ = 0.71073)
2θ range for data collection/°	4.176 to 56.744
Index ranges	-26 ≤ h ≤ 26, -25 ≤ k ≤ 25, -28 ≤ l ≤ 28
Reflections collected	99292
Independent reflections	19782 [R _{int} = 0.0702, R _{sigma} = 0.0645]
Data/restraints/parameters	19782/156/1104
Goodness-of-fit on F ²	1.023
Final R indexes [>=2σ (I)]	R ₁ = 0.0597, wR ₂ = 0.1330
Final R indexes [all data]	R ₁ = 0.1077, wR ₂ = 0.1583
Largest diff. peak/hole / e Å ⁻³	1.35/-1.03

Table S3. Crystallographic parameters for the structure of [Cr(BPOMe)₂]PF₆ (**3**).

Empirical formula	C40H32CrF6N10O4P
Formula weight	913.72
Temperature/K	100
Crystal system	triclinic
Space group	P1
a/Å	8.9680(9)
b/Å	11.1217(11)
c/Å	11.4442(11)
α/°	112.540(4)
β/°	110.284(4)
γ/°	96.764(4)
Volume/Å ³	946.57(17)
Z	1
ρ _{calc} g/cm ³	1.603
μ/mm ⁻¹	3.669
F(000)	467.0
Crystal size/mm ³	0.45 × 0.32 × 0.06
Radiation	CuKα (λ = 1.54178)
2θ range for data collection/°	8.994 to 136.774
Index ranges	-10 ≤ h ≤ 10, -12 ≤ k ≤ 13, -13 ≤ l ≤ 13
Reflections collected	23582
Independent reflections	6697 [R _{int} = 0.0568, R _{sigma} = 0.0569]
Data/restraints/parameters	6697/3/564
Goodness-of-fit on F ²	1.036
Final R indexes [>=2σ (I)]	R ₁ = 0.0709, wR ₂ = 0.1969
Final R indexes [all data]	R ₁ = 0.0713, wR ₂ = 0.1981
Largest diff. peak/hole / e Å ⁻³	0.79/-0.90

Table S4. Crystallographic parameters for the structure of [Cr(BPINMe₂)₂]PF₆ (**4**).

Empirical formula	C ₄₇ H ₅₀ Cl ₆ CrF ₆ N ₁₄ P
Formula weight	1220.68
Temperature/K	100
Crystal system	triclinic
Space group	P-1
a/Å	16.2168(14)
b/Å	17.7781(14)
c/Å	19.4572(16)
α/°	73.632(3)
β/°	88.899(3)
γ/°	76.362(2)
Volume/Å ³	5223.8(8)
Z	4
ρ _{calc} g/cm ³	1.552
μ/mm ⁻¹	0.629
F(000)	2500
Crystal size/mm ³	0.41 × 0.18 × 0.16
Radiation	MoKα (λ = 0.71073)
2θ range for data collection/°	4.78 to 55.434
Index ranges	-21 ≤ h ≤ 21, -21 ≤ k ≤ 23, 0 ≤ l ≤ 25
Reflections collected	36187
Independent reflections	36187 [R _{int} = 0.0735, R _{sigma} = 0.0963]
Data/restraints/parameters	36187/152/1438
Goodness-of-fit on F ²	1.04
Final R indexes [>=2σ (I)]	R ₁ = 0.0816, wR ₂ = 0.1980
Final R indexes [all data]	R ₁ = 0.1309, wR ₂ = 0.2311
Largest diff. peak/hole / e Å ⁻³	0.95/-1.01

Table S5. Crystallographic parameters for the structure of $[\text{Cr}(m\text{-BPIOMe})_2]\text{PF}_6$ (**5**).

Empirical formula	$\text{C}_{40}\text{H}_{32.69}\text{CrF}_6\text{N}_{10}\text{O}_{4.34}\text{P}$
Formula weight	919.94
Temperature/K	100
Crystal system	monoclinic
Space group	$\text{P}2_1/\text{c}$
a/Å	12.7669(7)
b/Å	20.9991(12)
c/Å	15.8721(9)
$\alpha/^\circ$	90
$\beta/^\circ$	106.583(2)
$\gamma/^\circ$	90
Volume/Å ³	4078.2(4)
Z	4
$\rho_{\text{calc}}\text{g/cm}^3$	1.498
μ/mm^{-1}	3.417
F(000)	1882
Crystal size/mm ³	0.38 × 0.36 × 0.22
Radiation	$\text{CuK}\alpha$ ($\lambda = 1.54178$)
2θ range for data collection/°	7.176 to 136.954
Index ranges	-15 ≤ h ≤ 15, -25 ≤ k ≤ 25, -18 ≤ l ≤ 19
Reflections collected	76035
Independent reflections	7491 [$R_{\text{int}} = 0.0546$, $R_{\text{sigma}} = 0.0260$]
Data/restraints/parameters	7491/0/576
Goodness-of-fit on F^2	1.039
Final R indexes [$ I \geq 2\sigma(I)$]	$R_1 = 0.0357$, $wR_2 = 0.0979$
Final R indexes [all data]	$R_1 = 0.0369$, $wR_2 = 0.0989$
Largest diff. peak/hole / e Å ⁻³	0.79/-0.45

Table S6. Selected bond lengths and bond angles obtained from crystallographic data for complexes **1–5**.

Complex		1	2	3	4	5	
Bond Angles (°)	N(imido)–Cr–N(imido)	176.1(8)	178.09(9)	179.74(16)	179.29(17)	177.61(6)	
	N(pyridine)–Cr–N(pyridine)	171.8(6)	173.67(9)	172.20(14)	174.93(17)	174.62(6)	
		171.8(6)	174.75(9)	173.18(14)	175.04(16)	175.05(6)	
	Cr–N(imido)	1.997(15)	1.981(2)	1.965(3)	1.985(4)	1.9856(14)	
		1.997(15)	1.985(2)	1.975(3)	1.986(4)	1.9903(14)	
	Cr–N(pyridine)	2.095(14)	2.099(2)	2.062(4)	2.098(4)	2.1158(15)	
Bond Lengths (Å)		2.095(13)	2.108(2)	2.070(3)	2.088(4)	2.0996(14)	
		2.125(14)	2.111(2)	2.083(3)	2.094(4)	2.0932(14)	
		2.125(14)	2.090(2)	2.084(3)	2.093(4)	2.0998(14)	

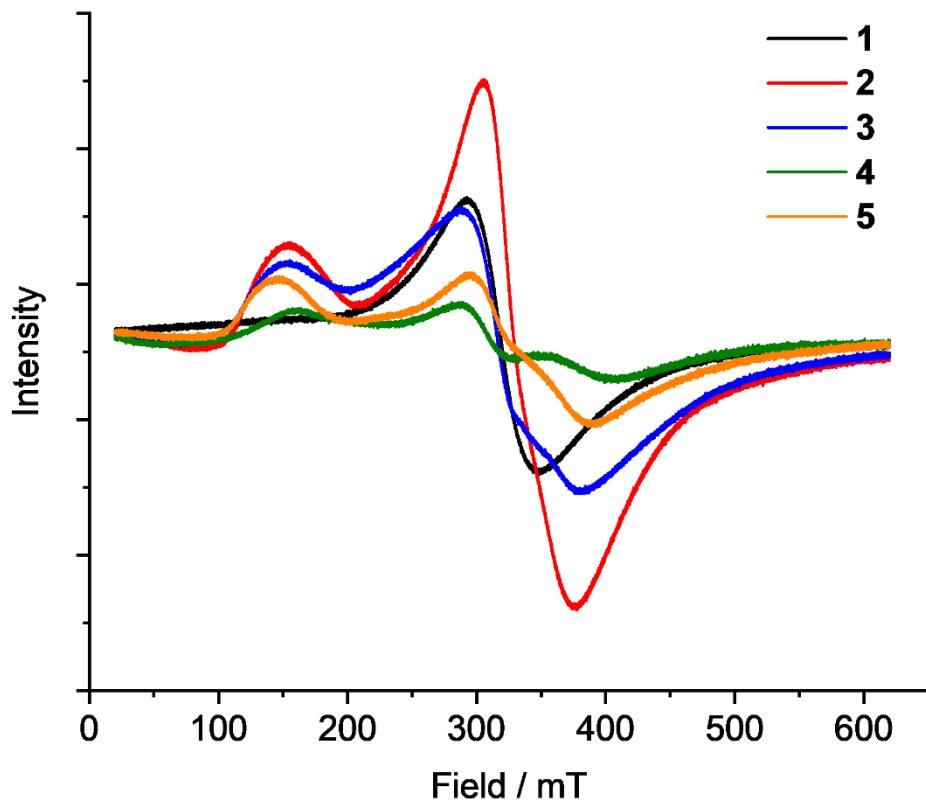


Figure S12. EPR spectra of complexes **1–5** in frozen CH_3CN ($5 \times 10^{-3} \text{ M}$) at 100 K.

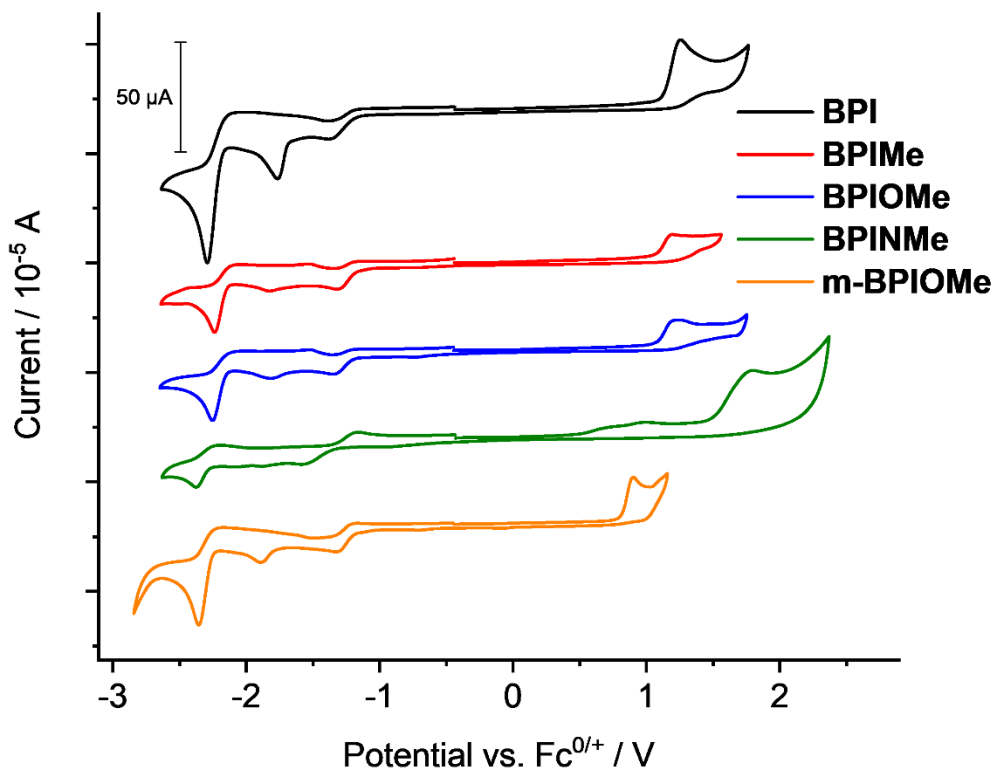


Figure S13. Cyclic voltammogram of the ligand precursors, in acetonitrile with 0.1 M ${}^n\text{Bu}_4\text{NPF}_6$ as supporting electrolyte, glassy carbon as working electrode. The scan rate was 50 mV/s.

Table S7. Redox potentials of complexes **1–5**.

Complex	Substituents	4σ	$E_{1/2} / \text{V vs. Fc}^{+/0}$				
1	R ¹ = H, R ² = H	0	−1.00	−1.25	−1.54	−1.85	−2.09
2	R ¹ = Me, R ² = H	−0.68	−1.09	−1.26	−1.59	−1.90	−2.14
3	R ¹ = OMe, R ² = H	−1.08	−1.22	−1.56	−1.87	−2.10	/
4	R ¹ = NMe ₂ , R ² = H	−3.32	−1.26	−1.51	−1.77	−2.10	/
5	R ¹ = H, R ² = OMe	0.48	−1.01	−1.26	−1.68	−1.97	−2.24

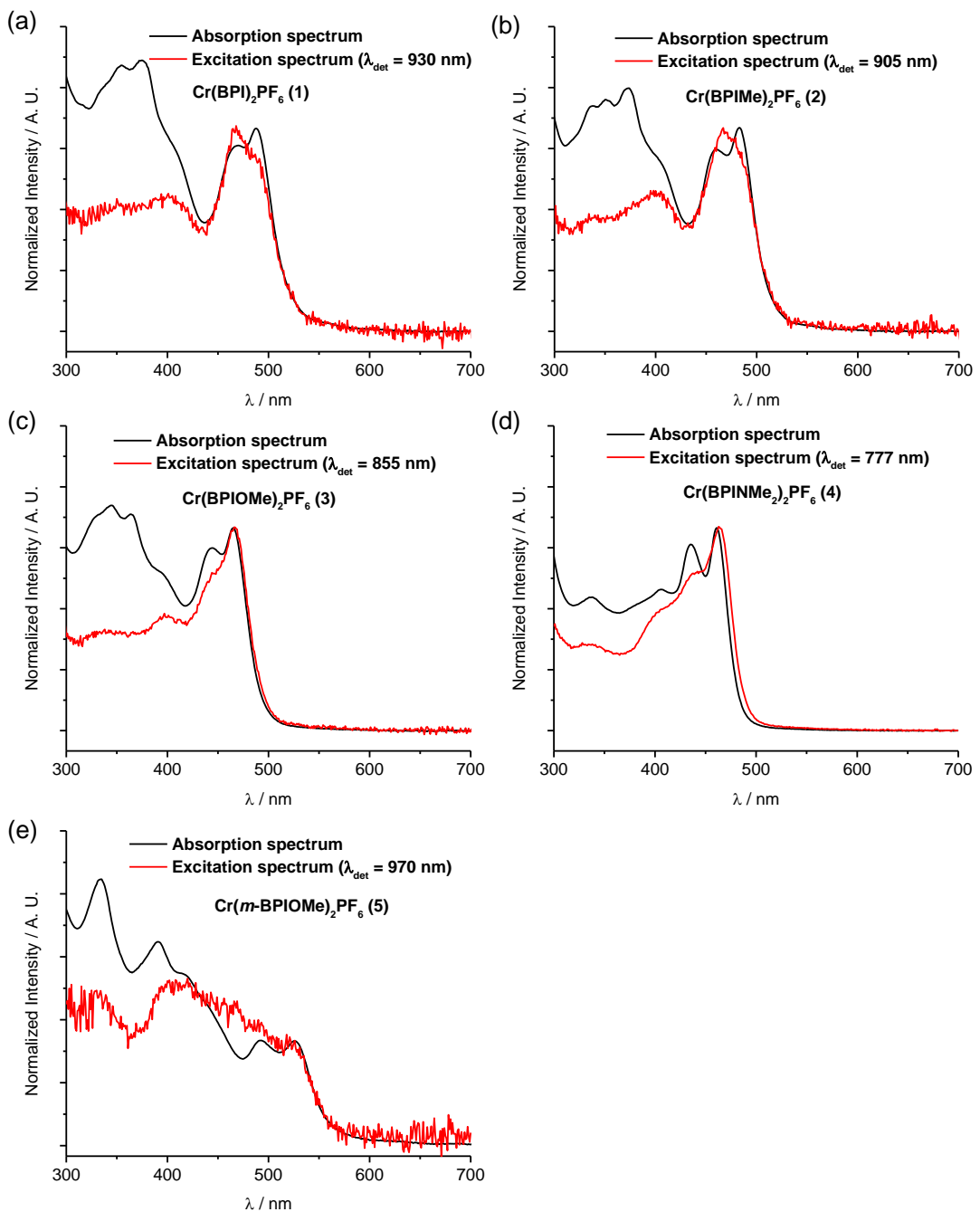


Figure S14. Excitation spectra and absorption spectra of complexes **1–5** in CH_3CN (concentration $1 \times 10^{-5} \text{ M}$).

Table S8. UV-vis absorption data of complexes **1–5** (1×10^{-5} M in CH₃CN at 298 K).

Complex	$\lambda_{\text{max}} / \text{nm} (\epsilon / \text{dm}^3 \text{ mol}^{-1} \text{ cm}^{-1})$
1	234 (53055); 257 (57214); 286 (sh, 29923); 336 (sh, 23528) 355 (25733); 375 (26223); 407 (sh, 17746) 470 (17984); 488 (19629)
2	237 (sh, 58541); 256 (65477); 290 (sh, 28577); 338 (24663); 351 (25340); 374 (26597); 404 (sh, 18688); 460 (19900); 483 (22284)
3	233 (sh, 60830); 252 (85020); 280 (sh, 43287); 328 (sh, 28047); 345 (29654); 364 (28487); 395 (20704); 444 (24042); 465 (26683)
4	249 (95900); 280 (73358); 337 (33144); 406 (35128); 435 (46300); 462 (50425)
5	238 (56897); 255 (61023); 281 (sh, 34072); 335 (32639); 391 (24973); 418 (sh, 20918); 493 (12885); 526 (12825)

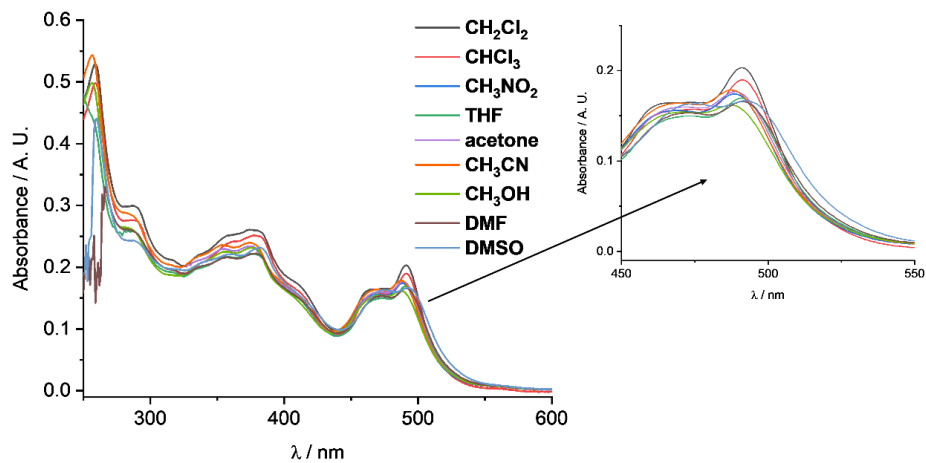


Figure S15. UV-vis absorption spectra of complex **1** in different solvents
(concentration 1×10^{-5} M).

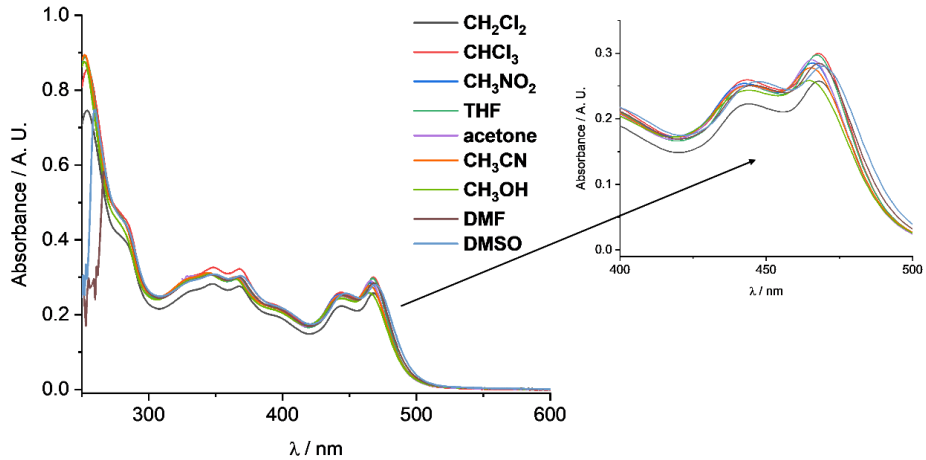


Figure S16. UV-vis absorption spectra of complex **3** in different solvents
(concentration 1×10^{-5} M).

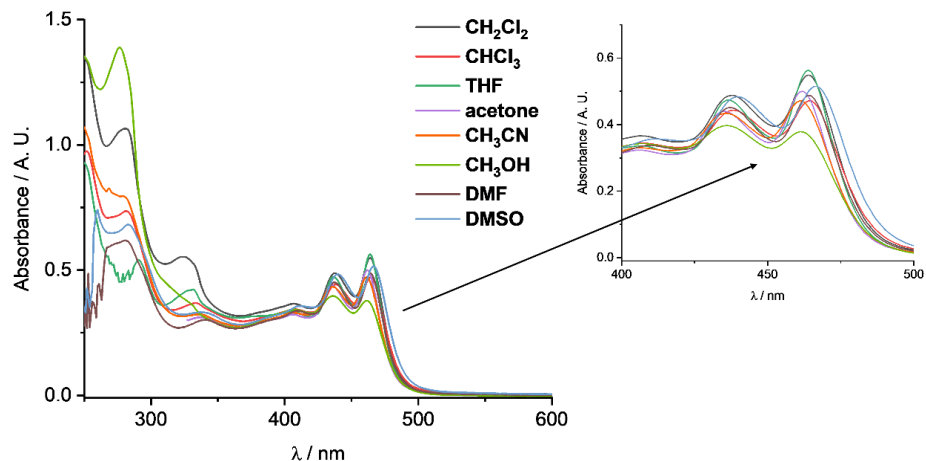


Figure S17. UV-vis absorption spectra of complex **4** in different solvents
(concentration 1×10^{-5} M).

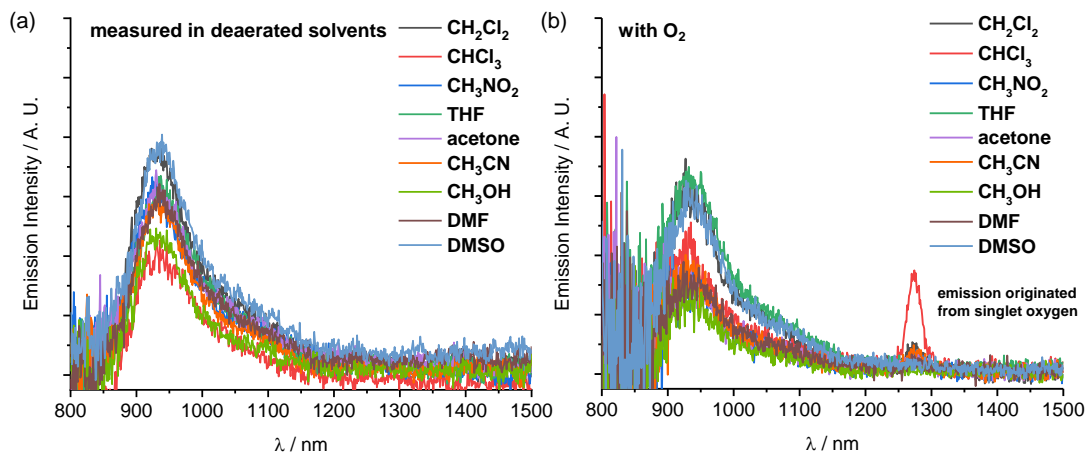


Figure S18. Emission spectra of complex **1** in different solvents (concentration 1×10^{-5} M) at 298 K upon excitation at 510 nm.

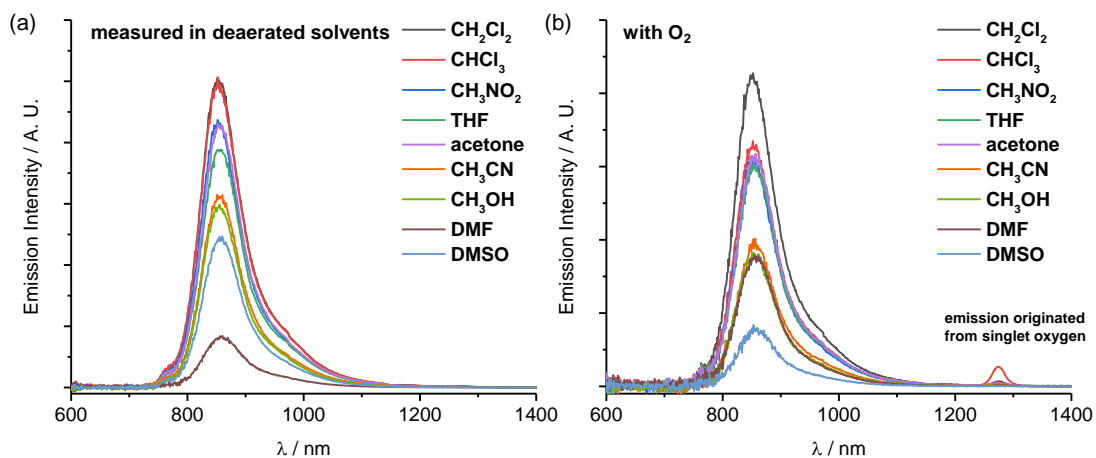


Figure S19. Emission spectra of complex **3** in different solvents (concentration 1×10^{-5} M) at 298 K upon excitation at 465 nm.

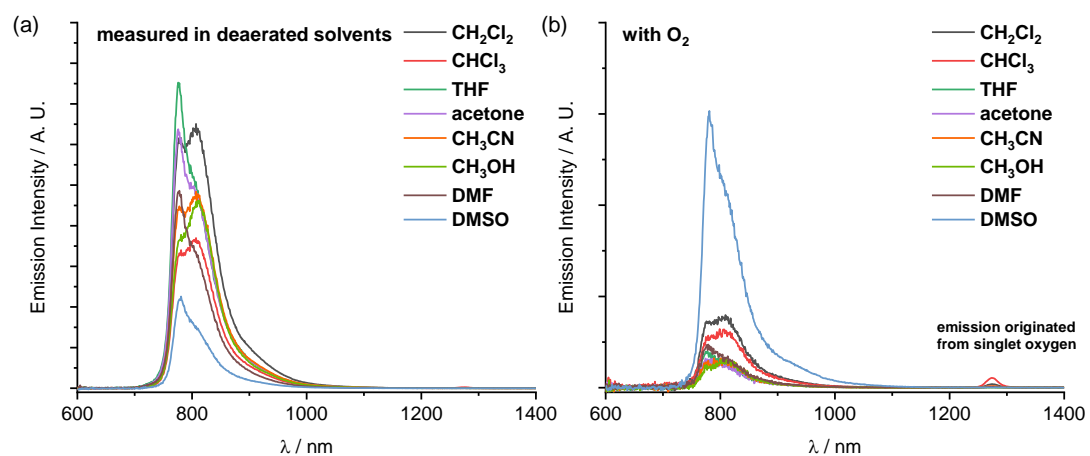


Figure S20. Emission spectra of complex **4** in different solvents (concentration 1×10^{-5} M) at 298 K upon excitation at 480 nm.

Table S9. Lifetime and QY of complex **4** in different solvents (concentration 1×10^{-5} M) at 298 K upon excitation at 480 nm.

Solvents	τ at 298 K / μ s		QY (%)
CH_2Cl_2	367.92 (777 nm)	371.68 (807 nm)	6.6
CHCl_3	110.27 (780 nm)	58.47 (780 nm)	3.9
THF	303.63 (777 nm)	299.85 (807 nm)	5.9
acetone	324.91 (777 nm)	329.40 (807 nm)	5.8
CH_3CN	310.01 (777 nm)	312.52 (807 nm)	5.9
CH_3OH	300.67 (780 nm)	297.78 (810nm)	4.2
DMF	291.31 (777 nm)	292.83 (807 nm)	5.8
DMSO	74.10 (777 nm)	72.68 (807 nm)	2.0

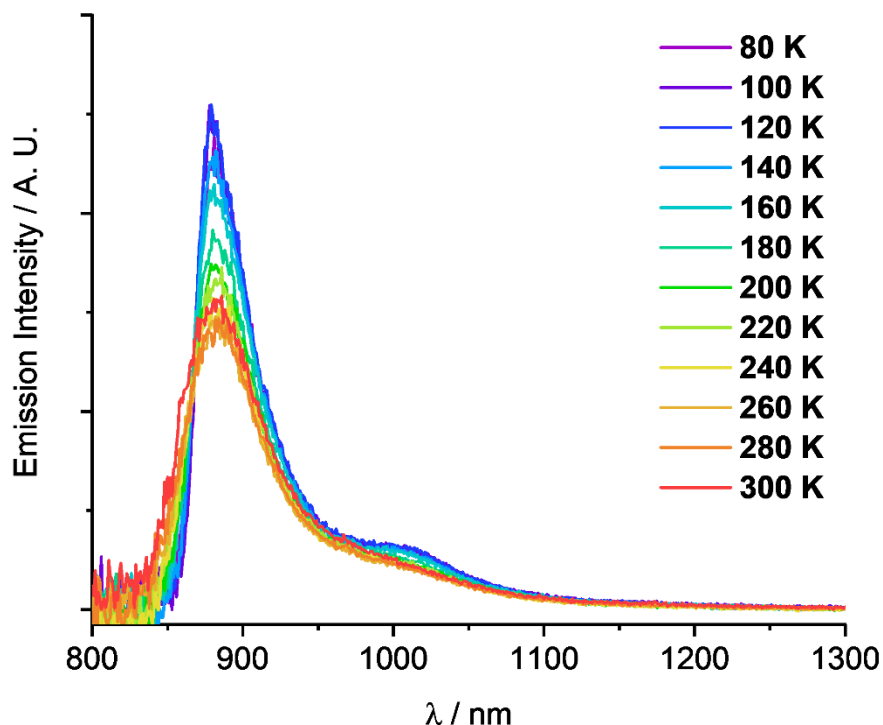


Figure S21. Temperature dependent emission spectra of complex **3** in solid state (80 K–300 K) upon excitation at 400 nm.

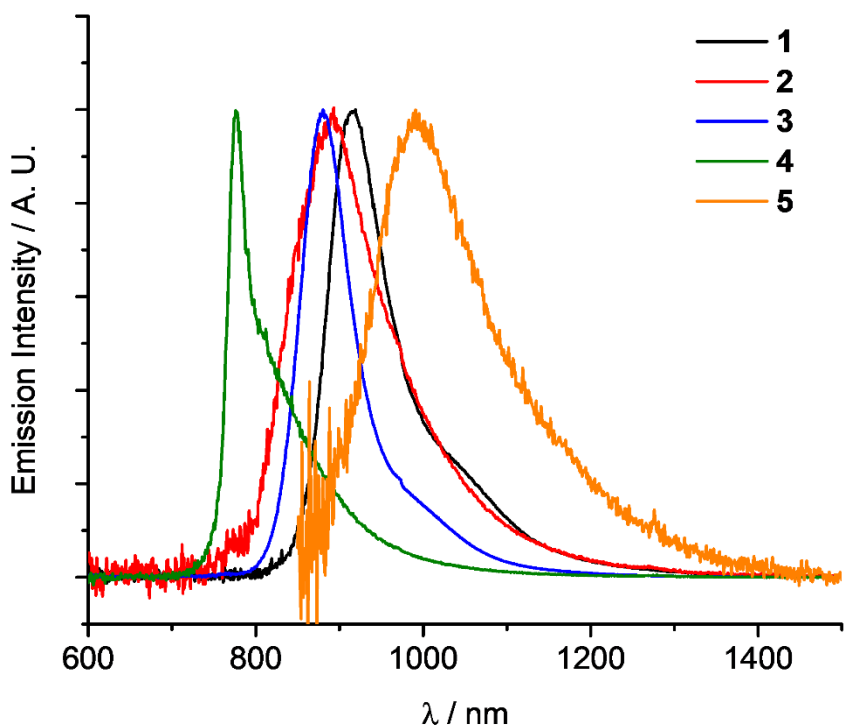


Figure S22. Emission spectra of **1–5** in solid state at 298 K upon excitation at 465 nm.

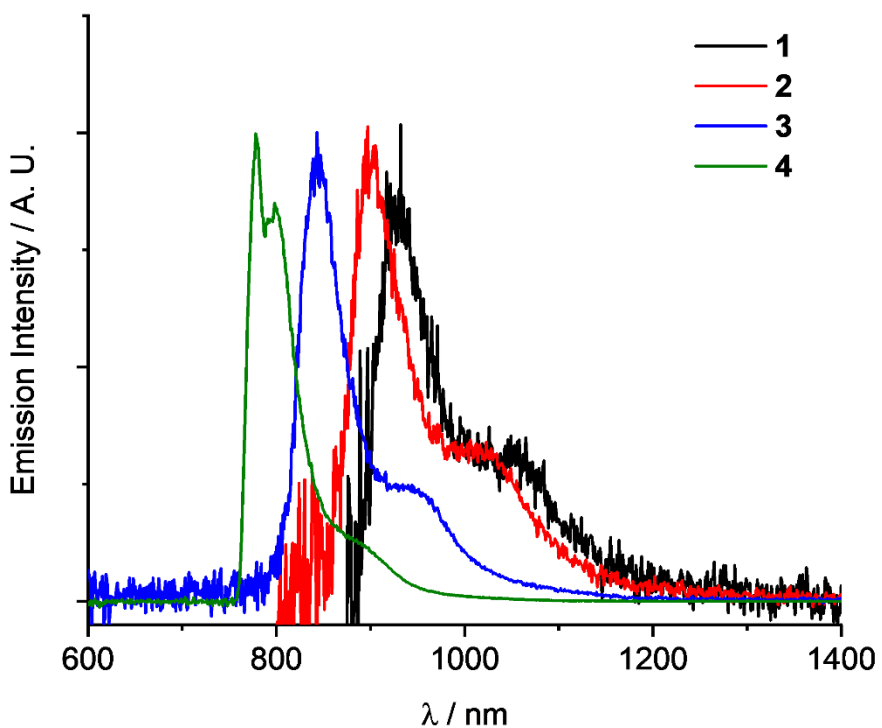


Figure S23. Emission spectra of **1–4** in 2-methyltetrahydrofuran glasses

(concentration 1×10^{-5} M) at 77 K, the emission signal of complex **5** is too noisy to distinguish.

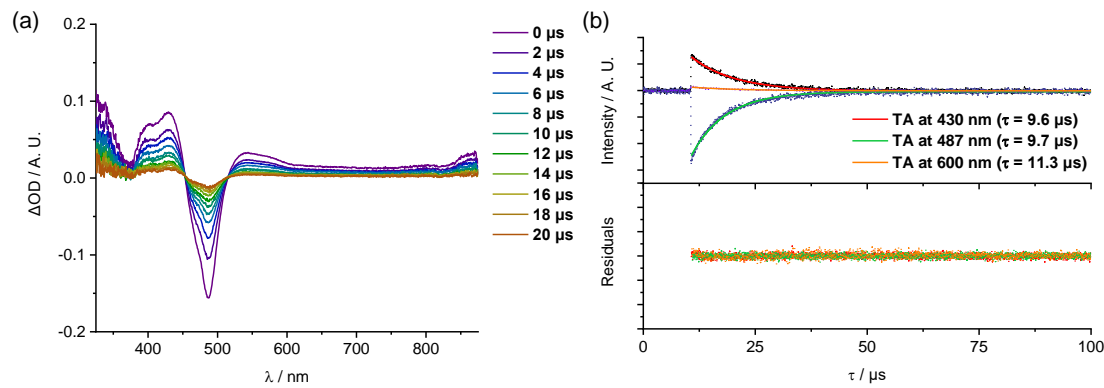


Figure S24. Time-resolved transient absorption (TA) spectra (a) and kinetic decays (b) of complex **1** (1×10⁻⁴ M in deaerated CH₃CN) recorded at 298 K upon excited with 355 nm pump laser pulses.

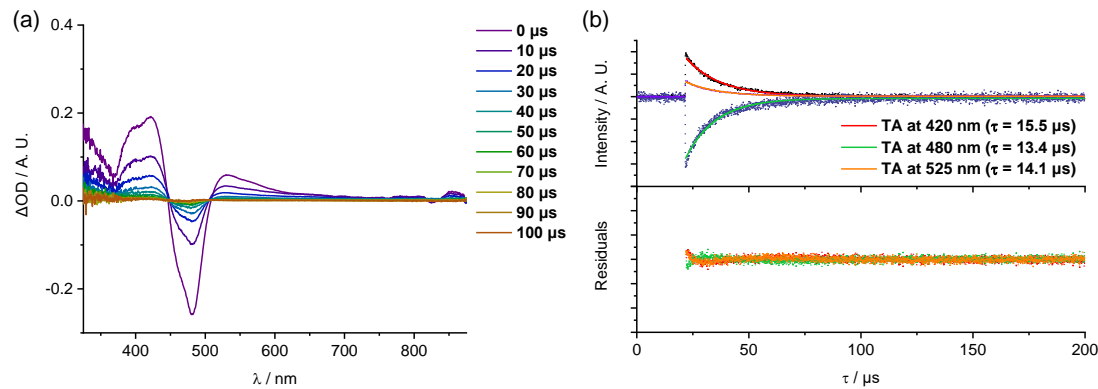


Figure S25. Time-resolved transient absorption (TA) spectra (a) and kinetic decays (b) of complex **2** (1×10⁻⁴ M in deaerated CH₃CN) recorded at 298 K upon excited with 355 nm pump laser pulses.

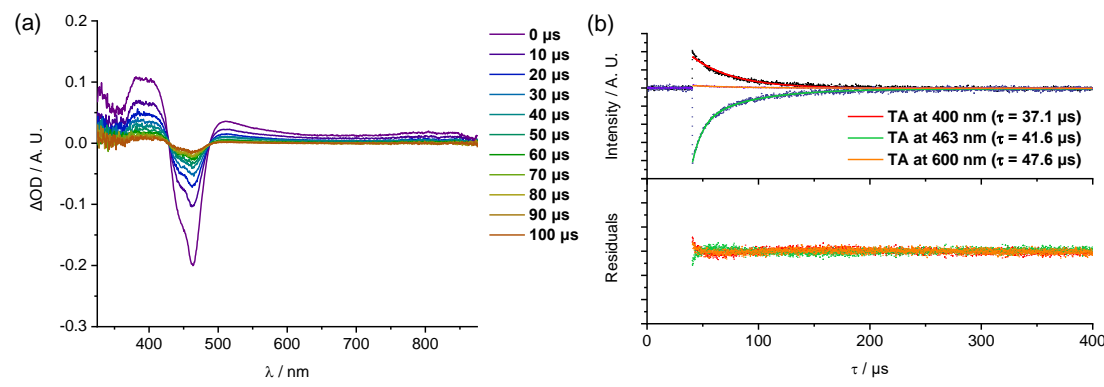


Figure S26. Time-resolved transient absorption (TA) spectra (a) and kinetic decays (b) of complex **3** (1×10⁻⁴ M in deaerated CH₃CN) recorded at 298 K upon excited with 355 nm pump laser pulses.

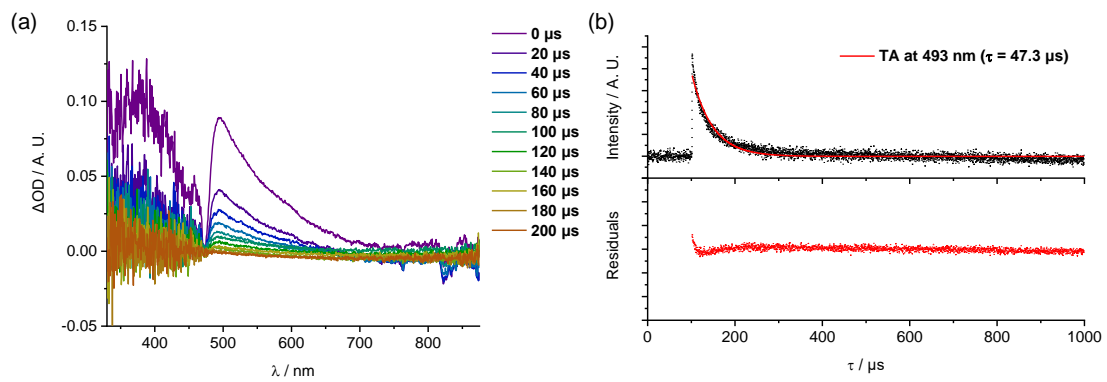


Figure S27. Time-resolved transient absorption (TA) spectra (a) and kinetic decays (b) of complex **4** (1×10^{-4} M in deaerated CH₃CN) recorded at 298 K upon excited with 355 nm pump laser pulses.

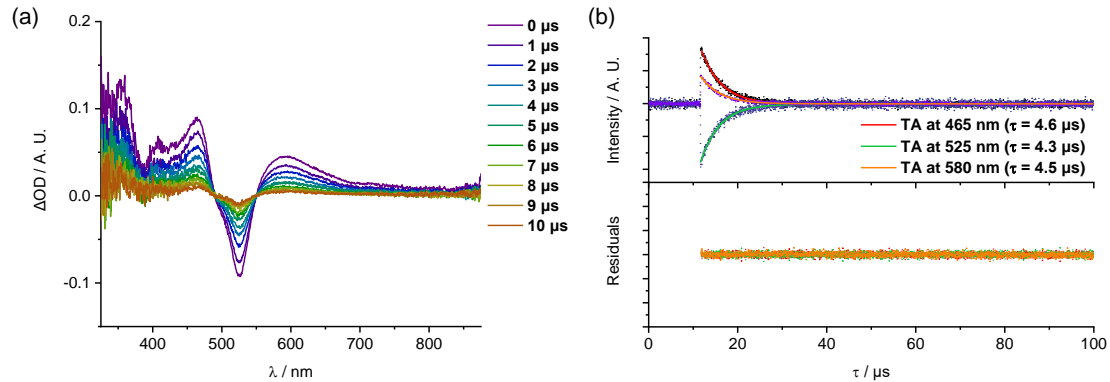


Figure S28. Time-resolved transient absorption (TA) spectra (a) and kinetic decays (b) of complex **5** (1×10^{-4} M in deaerated CH₃CN) recorded at 298 K upon excited with 355 nm pump laser pulses.

References for the Supplementary Information

1. C. S. Sevov, S. L. Fisher, L. T. Thompson and M. S. Sanford, *J. Am. Chem. Soc.*, 2016, **138**, 15378.
2. B. K. Langlotz, J. Lloret Fillol, J. H. Gross, H. Wadeohl and L. H. Gade, *Chem. Eur. J.*, 2008, **14**, 10267.
3. W. O. Siegl, *J. Heterocycl. Chem.*, 1981, **18**, 1613.
4. A. Scheja, D. Baabe, D. Menzel, C. Pietzonka, P. Schweyen and M. Broring, *Chem. Eur. J.*, 2015, **21**, 14196.
5. O. V. Dolomanov, L. J. Bourhis, R. J. Gildea, J. A. K. Howard and H. Puschmann, *J. Appl. Cryst.*, 2009, **42**, 339.
6. G. Sheldrick, *Acta Cryst.*, 2015, **A71**, 3.
7. G. Sheldrick, *Acta Cryst.*, 2015, **C71**, 3.